Influence of microstructure and weld size on the mechanical behaviour of dissimilar AHSS resistance spot welds

V. H. Baltazar Hernandez*[1,2], M. L. Kuntz[1], M. I. Khan[1] and Y. Zhou[1]

Resistance spot welds were produced in dissimilar combinations of advanced high strength steels. A 600 MPa dual phase (DP) steel was welded to a high strength low alloy, a 780 MPa DP, and a 780 MPa transformation induced plasticity steel. The microstructure and mechanical properties were characterised using metallurgical techniques and lap shear and cross-tension testing. The results show that a pullout failure mode with improved mechanical properties is obtained when DP600 is paired with other advanced high strength steels, compared to the DP600 welded to itself, which is prone to interfacial failure and poor mechanical properties, given the same weld size. An in depth comparison of the interfacial to pullout failure transition in similar DP600 and DP780 and dissimilar DP600–DP780 welds was performed. The results show that the interfacial to pullout transition for the DP600–DP780 welds is significantly lower than with DP600 welded to itself. Increased fusion zone strength through dilution with the DP780 promotes button pullout at smaller weld sizes. Furthermore, it was observed that softening in the heat affected zone of DP780 promoted a pullout failure mode in that material.

Keywords: Advanced high strength steel, Resistance spot welding, Dissimilar weld, Mechanical properties, Weld size, Microstructure

Introduction

Resistance spot welding (RSW) is the most widely used method for joining sheet metal in the automotive industry. It is also the favoured process for joining new and emerging grades of advanced high strength steels (AHSS).[1] Advanced high strength steels have been gaining in popularity due to their inherent strength and ductility characteristics. The high strength is obtained through a two component final microstructure achieved by intercritical annealing. The final microstructure consists of ferrite plus a second phase, which in the case of dual phase (DP) steels is martensite. With sufficient alloying and subcritical holding, a metastable ferritebainite structure with significant amounts of retained austenite can be achieved. These steels are known as transformation induced plasticity (TRIP) because at higher strains, the retained austenite transforms to martensite, giving the material excellent work hardening characteristics that persist over a large amount of strain.[1] The weldability of these materials, however, has been an ongoing concern due to the high amounts of carbon and other austenite stabilisers, which can produce hard microstructures in the weld region where high cooling rates are encountered. Microstructural changes in the fusion zone (FZ) and surrounding heat affected zone (HAZ) affect the weld mechanical properties and need to be characterised, and their effects understood, to develop optimised welding procedures for these materials.

Microstructural transformations in resistance spot welds are highly dependent on material chemistry and process parameters.[2] For instance, needle like martensite,[3] bainite, and acicular and widmanstätten ferrite[4] have been observed in the FZ of DP600 steels. Additionally, martensite, bainite, acicular ferrite and tempered martensite were observed in the HAZ.[5] The heterogeneous nature of RSW and the wide range of expected microstructures make prediction of weld properties and failure modes difficult. The failure mode is a qualitative measure of mechanical properties and can be classified as: interfacial, partial interfacial and pullout.[6,7] It is well established that the weld size has a significant effect on failure mode and weld strength in spot welds,[8] with a pullout failure mode most desirable. The transition from interfacial to pullout failure modes can generally be linked to the increase in the weld size above some minimum value, which is known as the 'transition weld size'. Typically, the minimum weld size has been specified as a function of the sheet thickness; however, microstructure and hardness aspects have also been discussed.[9,10]

The expected failure mode can be approximated using a simplistic engineering approach. Interfacial failure is expected when the shear stress across the weld nugget

[1]Centre for Advanced Materials Joining, University of Waterloo, 200 University Avenue West, Waterloo, Ont. N2L3G1, Canada
[2]MPyM-EPMM Academic Unit of Engineering, Autonomous University of Zacatecas, 801 Ramon Lopez Velarde Avenue, Zacatecas 98000, Mexico

*Corresponding author, email v.h.baltazar@gmail.com

Received 23 March 2008; accepted 24 May 2008
DOI 10.1179/136217108X325470

exceeds the local strength; conversely, pullout failure is expected when the strength of the circumferential band of material running through the HAZ is exceeded first. In some cases of RSW in DP steels, the failure transition behaviour is orderly and predictable.[11] There have been several reports, however, of interfacial failures in DP600 steels when the weld size exceeded the expected threshold.[12] Such failures were attributed to solidification cracks and shrinkage voids.[13] Understanding the nature of RSW failure is usually straightforward when both sheets are of the same material and thickness; however, problems arise when one of the sheets consists of a different material, i.e. a dissimilar combination.

Most research has been directed at RSW of the same sheets being welded together, i.e. a similar combination. However, in many applications, spot welds are made between different materials and thicknesses as mechanical properties are tailored to local requirements. For instance, Kuo and Wexler[14] spot welded 1·8 mm DP600 to 2·2 mm HSLA350 using a design of experimental approach. Milititsky *et al.*[15] obtained a weld lobe for a three thickness stack-up, including DP600, HSLA and mild steel. In both studies, there was no attempt to compare the changes in failure mode among different combinations of AHSS. Svensson[16] developed predictions of FZ microstructure and hardness by estimating dilution in dissimilar combinations; however, weld properties and failure modes were not considered. The effect of microstructural evolution and its influence on the mechanical performance of AHSS in dissimilar combinations are relatively unknown.

The objective of this study is to analyse the influence of the post-weld microstructure and the weld size on the mechanical performance (failure location, failure modes and peak loads) of AHSS steel spot welds in combination with dissimilar steels. A DP600 was selected as a baseline for comparison due to its current popularity in automotive applications. The DP600 was welded in combination with a TRIP780, a DP780 and an HSLA to cover a wide range of potential joint combinations. In this work the following terminology is adopted: failure is the state of imminent through thickness fracture; and failure location is the sheet where fracture occurred.

Experimental

Materials

The steels used in this work are listed in Table 1. The AHSS includes: two DP steels (600 and 780 MPa) and one TRIP steel (780 MPa). An HSLA was also included due to its widespread application. The nominal sheet thickness was 1·2 mm, with a range of 1·0 mm in the TRIP780 to 1·2 mm in the DP600. The key alloying elements are listed in Table 1 along with the carbon equivalent (CE_Y) as calculated using Yurioka's equation.[17] The material combinations are shown in Table 2.

Welding process

Welds were conducted using a pedestal type, pneumatically controlled, 250 kVA single phase AC RSW machine with constant current control operating at 60 Hz. According to the Resistance Welding Manufacturing Alliance[18] (RWMA) the electrodes for welding were female, 40° truncated, class 2 type E with a 6 mm face diameter. Electrodes were cooled following AWS standards[19] with a water flow rate of 4 L min^{-1}. New electrodes were applied for each combination and a stabilisation procedure suggested by the AWS was employed to break in the contact tips. The squeeze time and hold time were kept constant at 25 and 5 cycles respectively. Thus, the electrodes were released from the work 5 cycles after the termination of weld current, this being a recognised standard feature of RSW procedures for sheet steel welding. The purpose of electrode release is to reduce the post-weld cooling rate. Single pulse welding schedules were used with starting parameters as shown in Table 2. The selected welding schedules were developed in previous work[20] and designed to produce a target weld size in excess of 5·5 mm, or $5(t)^{1/2}$, where t is the sheet thickness (1·2 mm), which is commonly used as a minimum set-up weld size.

Mechanical testing

The lap shear tension test and the cross-tension test were used to characterise the mechanical properties of the welds. The tensile tests were conducted with an Instron 4206 universal testing machine. Coupon dimensions for lap shear, cross-tension and peel testing were: 105×45, 150×50 and 120×40 mm respectively. Samples were prepared following AWS standards.[19] All tests were performed at room temperature. The crosshead velocity was maintained at a constant rate of 10 mm min^{-1}. Shims of same thickness bulk material were used for all specimens to maintain alignment in shear tensile testing. The test schematics are shown in Fig. 1*a* and *b*, for lap shear tension and cross-tension respectively. For comparison purpose among the dissimilar combinations, failure loads were normalised for sheet thickness and weld diameter. Weld diameter measurements were obtained from the failed cross-tension and lap shear samples and the normalised thickness was taken from the sheet in which failure occurred. Partial tensile tests were conducted by stopping the crosshead before final fracture of the specimen; in this case the tests were stopped at 2·0 and 2·4 mm of displacement.

Metallography and hardness testing

Metallographic cross-section samples were prepared and the weld microstructures were examined by optical

Table 1 Base metal properties

Steel	Thickness, mm	Coating		Alloying elements, wt-%					
		Type	Average weight, g m^{-2}	C	Mn	Mo	Cr	Si	CE_Y
HSLA	1·14	GI	77·8	0·080	0·830	0·010	0·030	0·450	0·183
DP600	1·2	HDGI	55·1	0·099	1·523	0·196	0·197	0·157	0·326
DP780	1·15	GA	58·8	0·113	2·082	0·181	0·239	0·036	0·427
TRIP780	1·0	GI	62·5	0·188	1·631	0·012	0·023	1·618	0·527

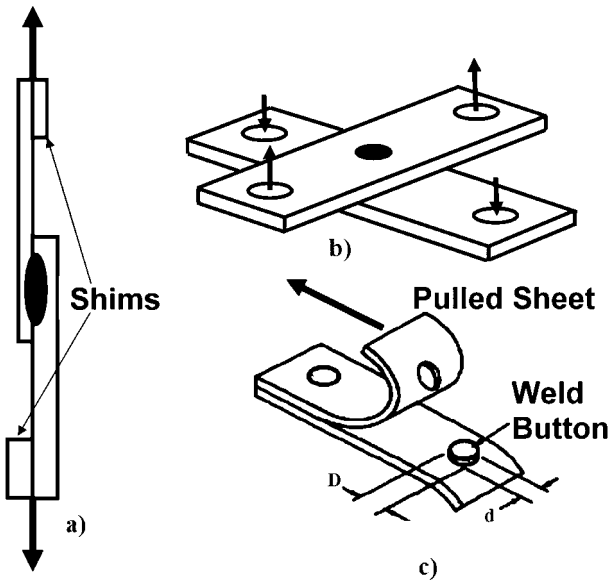

1 Mechanical testing schematic: *a* lap shear tensile, *b* cross-tension, *c* peel; black arrows indicate loading direction

microscopy and scanning electron microscopy (SEM). The partial tensile samples were sectioned parallel to the tensile direction along the centre of the weld. A nital etching reagent was used to reveal microstructures. Cross-weld hardness profiles were obtained at room temperature using a Vickers microhardness tester according to AWS standards.[19] An applied load of 200 g and a time of 15 s were used. The indentations were spaced 0·2 mm apart. The microhardness traverses were performed on a diagonal covering base metal (BM), HAZs and FZs of both steels.

Weld size measurement

Peel testing was used to measure the weld size, as per AWS specifications. Both sheets in the dissimilar material combination were peeled back in separate tests to have consistent measurements. The weld size was measured as an average of the minimum and maximum button dimensions, as depicted in Fig. 1*c*. In some cases weld size measurements from metallographic cross-sections were also made using image analysis. The weld size measurements are given in Table 3. A stereo microscope was used to measure the apparent fracture area as an indication of weld size of some lap shear interfacial failure welds.

Results and discussion

Microstructure and hardness distribution

Weld cross-sections for the three dissimilar steel combinations are shown in Fig. 2. The three distinct regions, including $BM_{1,2}$, $HAZ_{1,2}$ and FZ are labelled with the subscripts 1 and 2 referring to the DP600 and the pairing steel respectively.

Table 2 Welding schedules

Combination	Force, kN	Current, kA	Time, cycles
DP600–DP780	3·5	8·0	20
DP600–TRIP780	4·0	8·0	20
DP600–HSLA	3·5	8·5	20

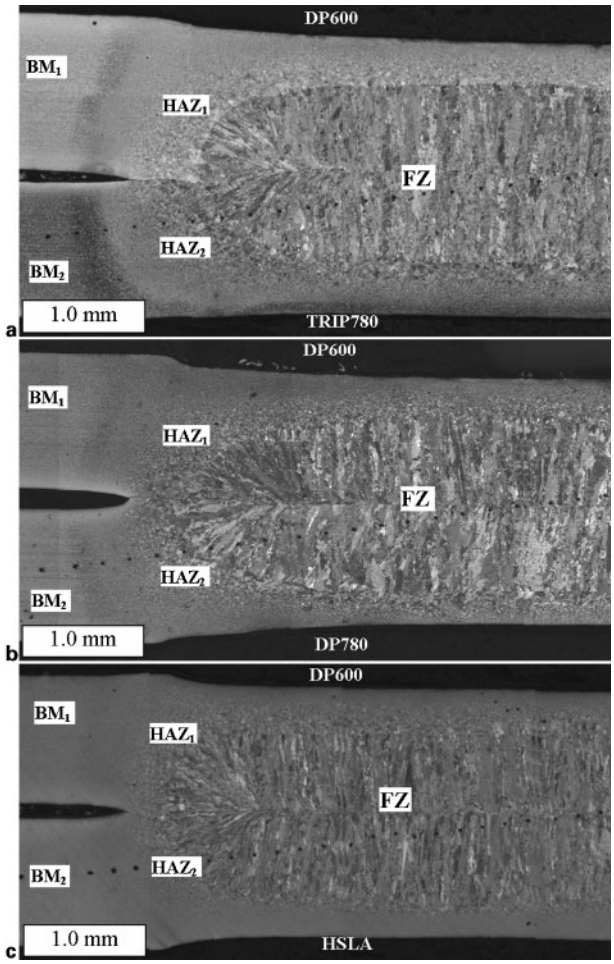

FZ – fusion zone, HAZ – heat affected zone and BM – base metal

2 Dissimilar spot weld cross-sections: *a* DP600–TRIP780, *b* DP600–DP780, *c* DP600–HSLA

Figure 3 shows the measured cross-weld hardness profiles. The DP600 steel was plotted to the left of the diagram for consistency. As shown in Fig. 3, the FZ hardness increased when DP600 was paired with increasingly highly alloyed steel from the lower grade HSLA to the higher steel grades DP780 and TRIP780. The average FZ hardness of each combination is listed in Table 4. The alloying level (i.e. CE_Y) listed in Table 1 increased in order of HSLA, DP600, DP780 and TRIP780. The trend of the average FZ hardness was to increase with increased alloying level (CE_Y) of the steel paired with the DP600. It was also noted that within each dissimilar weld nugget the hardness was quite constant along the diagonal path, suggesting that the welding process was able to thoroughly mix the liquid metals originating from the respective steels.

It was noted from Fig. 3 that the FZ hardness of each combination was between the peak hardnesses in the HAZ of the respective steels. For example, the FZ

Table 3 Weld size, mm

Steel combination	Peel test	Metallographic cross-section
DP600–TRIP780	6·2±0·3	6·0±0·2
DP600–DP780	5·9±0·1	5·9±0·2
DP600–HSLA	6·2±0·3	5·3±0·4

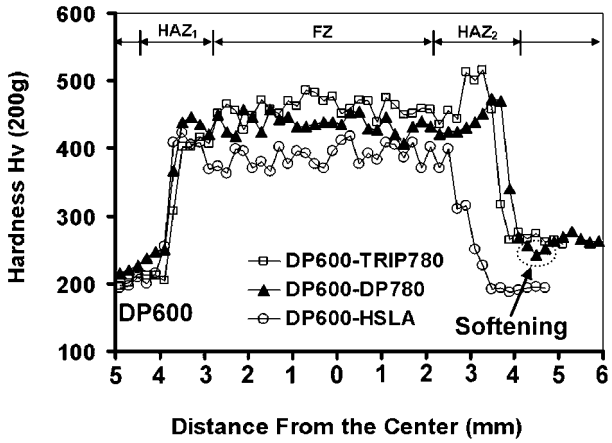

3 Cross-weld hardness profile for dissimilar spot welds

hardness of the DP600–TRIP780 (460 HV) was between the peak HAZ hardness of the DP600 and TRIP780 (410 and 500 HV respectively). Furthermore, the peak HAZ hardness values were similar to those observed in RSW of the steels to themselves.[6] Observable softening was found in the outer, subcritical HAZ of the DP780, where the local hardness of 240 HV was lower than the BM hardness (267 HV) as a result of martensite tempering. The increased volume fraction of martensite in DP780 BM microstructure resulted in a measurable decrease in hardness in this region, while in the DP600 or TRIP780 the lower BM martensite content did not present any measurable softening in microhardness testing. Softening was not observed in the HAZ of the HSLA.

The FZ microstructure for each weld combination is shown in Fig. 4. The predominantly martensitic microstructures showed directional, columnar solidification from the fusion boundary towards the centre in all combinations. Figure 4*a* and *b* shows a nearly fully martensitic FZ microstru\cture for the DP600 paired to the TRIP780 and the DP780 respectively. The DP600–HSLA FZ microstructure, as shown in Fig. 4*c*, consists partly of sideplate ferrite structures, of a widmanstatten character, growing from the prior austenite grain boundaries, in addition to lower temperature bainitic and martensitic products. Overall, the observed FZ microstructures correlated well with the FZ hardness trends.

Joint strength and failure location

Figures 5 and 6 show representative fracture surfaces for the cross-tension and lap shear tensile tests respectively. The average normalised peak loads to failure are shown in Fig. 7, with the dissimilar DP600 combinations increasing in steel grade from left to right. Under cross-tension loading, the failure was consistently located in the higher grade steel of the combination, as listed in Table 5. The fracture path was through the harder HAZ, as shown in Fig. 5*a–c*. Normalised peak cross-tension loads shown in Fig. 7 were the highest in

Table 4 Fusion zone hardness

Dissimilar combination	Fusion zone hardness,HV	Standard deviation
DP600–TRIP780	460	14·11
DP600–DP780	435	12·98
DP600–HSLA	388	15·77

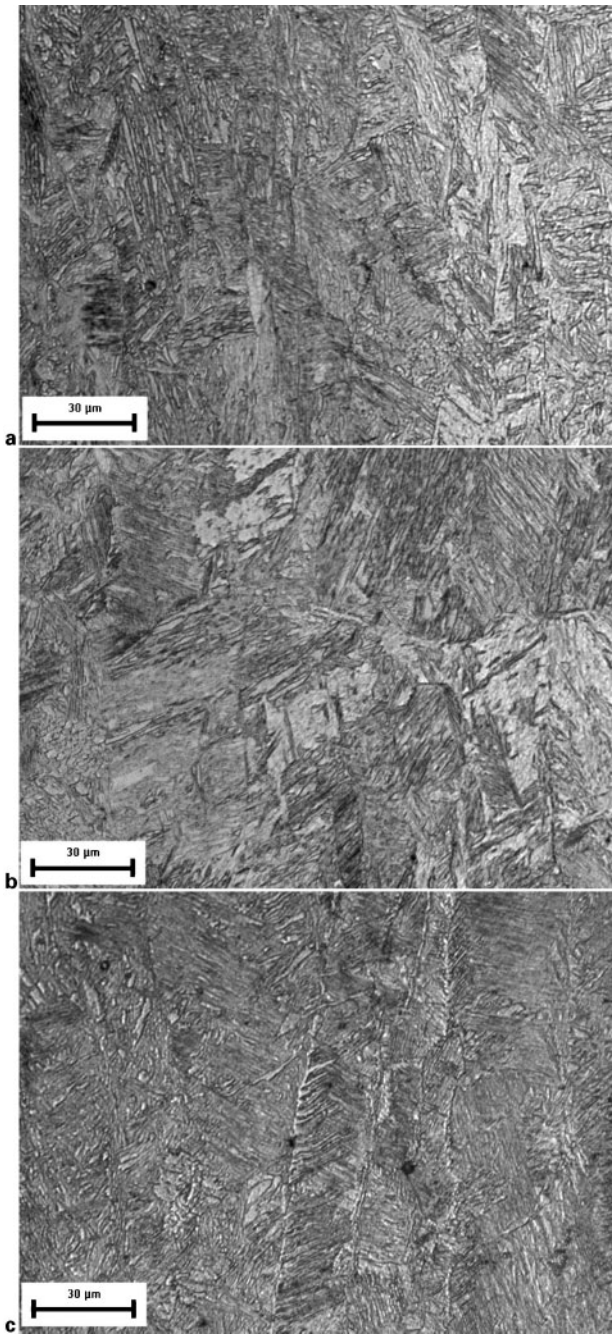

4 Fusion zone microstructures: *a* DP600–TRIP780, *b* DP600–DP780 and *c* DP600–HSLA

the DP600–HSLA combination, and decreased in order of DP600–DP780 and DP600–TRIP780. A general trend of decreasing cross-tension strength with increasing steel grade in combination with the DP600 was observed. Comparable results have been reported for RSW of steels with tensile strengths of 300 to 1250 MPa when welded to themselves.[21]

With the weld sizes produced by the procedures in Table 2, lap shear tensile test results produced a full button pullout failure mode for all of the dissimilar combinations, as shown in Fig. 6. The failure locations, listed in Table 5, revealed no general trends. For instance, in the DP600-HSLA combination, failure occurred outside of the HAZ, in the HSLA base metal, as shown in Fig. 6(a). Final fracture in the DP600-DP780 weld occurred in the DP780 HAZ softened zone;

5 Cross-tension test failures

however, a double-thickness failure was observed, as shown in Fig. 6(b), where fracture also occurred within the HAZ of the DP600. The double thickness failure was a feature unique to this combination. In Fig. 6*c* the DP600–TRIP780 weld failed along the fusion boundary at the TRIP780 HAZ. Similar results involving TRIP steel have also been reported.[20] Figure 7 shows a general trend of increasing normalised peak shear tensile loads with increasing steel grade combinations.

Previous work has shown that in the 1·2 mm thick DP600, interfacial failures in lap shear testing occurred with a similar target weld size (i.e. 5·5 mm, or $5(t)^{1/2}$).[3] In the present work, however, full button pullout failures were observed when the same DP600 was paired with other steels given the same setup weld size. In particular, the DP600–DP780 combination produced high failure loads in both cross-tension and lap shear testing. The DP600–DP780 combination was also interesting because it produced a double thickness failure in both sheets in the lap shear tensile loading condition. Thus, the DP600–DP780 combination was selected as a basis for further comparison of the effects of welding conditions and weld size on failure characteristics in similar *v.* dissimilar stack-ups, which is detailed in the remainder of the paper.

Failure mode transition

It is well known that the strength and failure characteristics of spot welds are functions of the nugget size, sheet thickness and weld/HAZ hardness.[9,10,13] From a basic stress analysis, it can be shown that the transition from interfacial failure to pullout failure occurs when the weld size exceeds a critical value.[11,22] Some materials, DP600 in particular, have shown interfacial failure at weld sizes that are above the recommended minimum.[6] However, observations in this work have shown that the interfacial failure mode for a DP600 steel changes to a pullout failure mode when welded in combination with dissimilar steels, given the same weld size.

An RSW growth curve, shown in Fig. 8, shows the effect of increasing current on weld size, as measured using the peel test, for similar (DP600 and DP780) and dissimilar (DP600–DP780) welds, with constant weld time and force of 20 cycles and 3·5 kN respectively. There was little effect of material combination on the relationship between weld size and current; however, the results were subject to some inaccuracy due to the effects of HAZ material present around the button periphery, which was not consistent for each combination. Regardless, the relationship between weld size and current is clearly established in Fig. 8.

In Fig. 9, the tensile strength *v.* weld current is given upon a force of 3·5 kN and 20 cycles for weld time. Figure 9*a* shows the dissimilar DP600–DP780 combination. Pullout failures were identified by the solid graph symbols. From the results, it is apparent that the transition from an interfacial to a pullout failure mode occurs between 7·5 and 8 kA. The transition occurred at a peak load of 15·7 kN. From reference to Fig. 8, it can be said that the transition weld size is $\sim$5·5 mm. This was confirmed by visual inspection of the interfacial failure fracture surface diameters at the transition point, which averaged 5·3 mm. Figure 9*b* and *c* shows results for the similar material welds in DP600 and DP780 respectively. In DP600 welds, the transition from interfacial failure to pullout failure occurred over a

6 Lap shear tensile failures

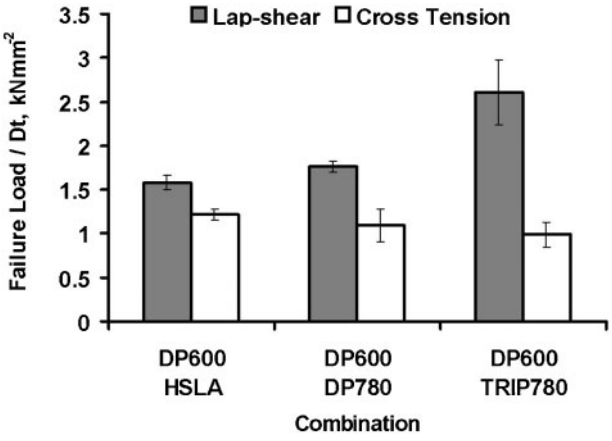

7 Mechanical testing results for lap shear and cross-tension loading conditions

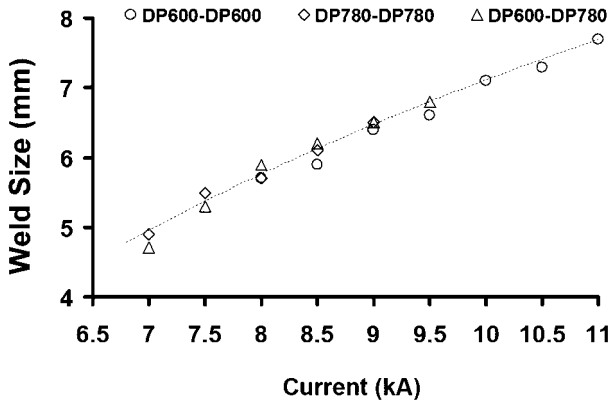

8 Weld growth curve for similar (DP600 and DP780) and dissimilar (DP600–DP780) weld stack-ups

range of 8·5 to 9·5 kA. The transition was marked by a failure load of 15·6 kN. Correlation with Fig. 8 shows that the transition weld size is around 6 to 7 mm. Visual inspection of the interfacial fracture surfaces at the transition point gave an average weld size of 6·1 mm. For the DP780 welds, the transition occurred from 7·5 to 8 kA, corresponding to a weld size of $\sim$5·5 mm and a peak load of 17·3 kN. From the interfacial fracture surfaces, the transition diameter was greater than the average of 5·7 mm. The scatter in the results in Fig. 9*a–c* is most likely due to random variation in weld size for welds produced at constant settings, which is common in RSW. The notable feature on these charts was that the transition peak load was clearly demarcated in the results and was apparently related to a constant transition weld size.

The DP600–DP600 welds showed the highest transition weld size at 6·1 mm, which is well above the $5(t)^{1/2}$ set-up weld size of 5·5 mm, and significantly more than the $4(t)^{1/2}$ minimum weld size of 4·5 mm that is commonly specified. These results are consistent with what has been observed in previous work which has claimed that interfacial failures were common in DP600 even when the weld size exceeded commonly used standards. In the DP780–DP780 welds, the transition weld size was found to be $\sim$5·7 mm, which still exceeds the specifications, but is significantly lower than the DP600. For the dissimilar DP600–DP780 combination, the transition size was found to be 5·3 mm, which was lower than both the DP600 and DP780 cases. Also worth noting is that at the transition point, the peak load of the DP600–DP600 and DP600–DP780 welds were the same at around 15·6–15·7 kN, while the peak load of the DP780–DP780 welds was higher at 17·3 kN.

Failure analysis

As previously explained, the transition from interfacial to pullout failure modes generally occurs when the stress in the HAZ exceeds the local yield strength. Increasing the weld size or FZ strength or the HAZ properties promotes this transition. In the cases above, the weld microstructure was predominately martensitic; however, bainite and tempered martensite were also thought to be

Table 5 Failure location

Combination	Cross-tension	Shear tensile
DP600–TRIP780	TRIP780	TRIP780
DP600–DP780	DP780	DP780/DP600
DP600–HSLA	DP600	HSLA

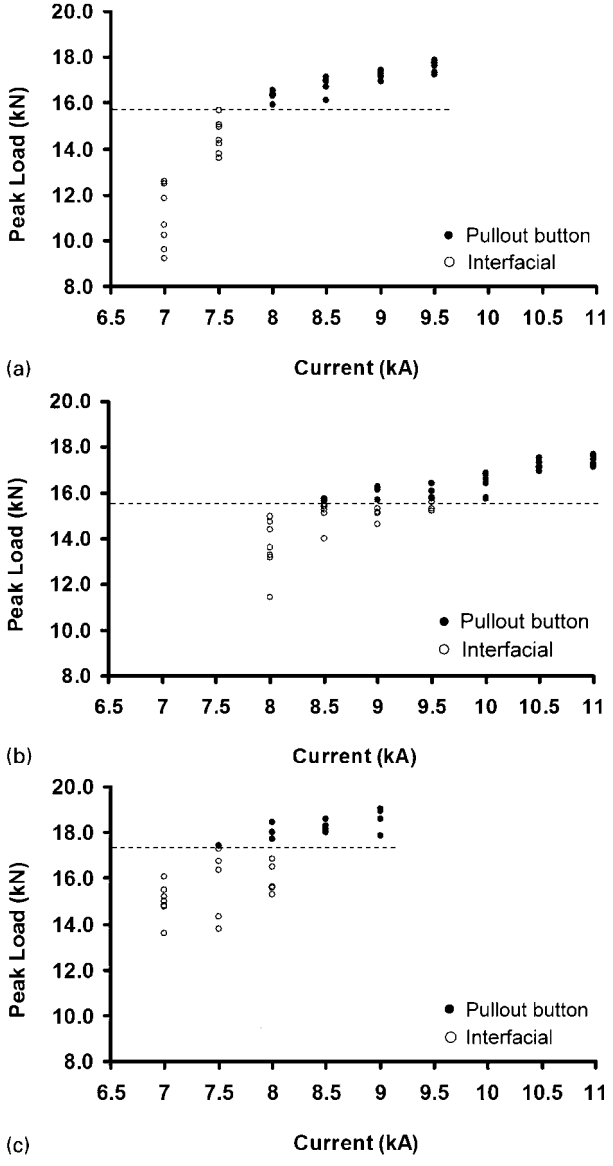

9 Peak load *v.* current at 3·5 kN electrode force and 20 cycle weld time: *a* DP600–DP780, *b* DP600–DP600 and *c* DP780–DP780

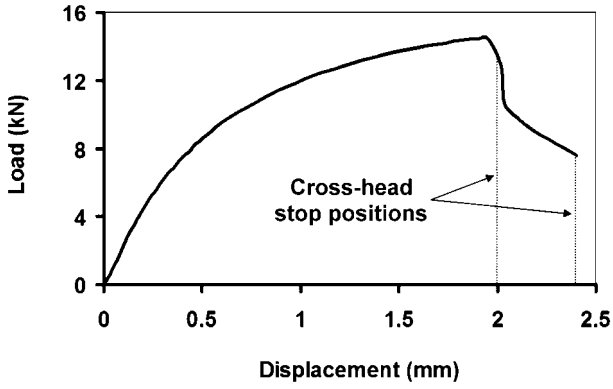

10 Partial lap shear tensile test load–displacement curve

present in some fraction. As shown in Fig. 3 the average FZ hardness of the DP600–DP780 weld was somewhere between the peak hardness in the DP780 HAZ, which was higher, and the peak hardness in the DP600 HAZ, which was lower. The final microstructure, hardness, and ultimately, strength of the FZ was a function of the alloying level (CE_Y), which is an indication of hardenability, and the C content, which is the primary factor in the hardness of martensite. The DP600 had a lower CE_Y (0·326) with a lower C content (0·099%) than the DP780 (CE_Y: 0·427 and C content: 0·113%), and thus had a lower hardness. Owing to mixing and dilution, the hardness of the DP600–DP780 FZ was between the two. Thus, it is reasonable to say that the FZ strength of the welds increased in the order of DP600–DP600, DP600–DP780 and DP780–DP780. This helps to explain why the transition weld size for the DP600 was higher.

It has been mentioned that the HAZ hardness is another factor in the transition weld size. The characteristic mechanisms of the button pullout failure mode in lap shear testing include rotation of the weld nugget, and stretching, thinning, and necking in the HAZ.[7,23] In fact, even though the loading condition is nominally shear, the failure mode is predominantly tensile through rotation and preferential necking in the ductile region of the HAZ.[22] In the DP600–DP780 combination, partial

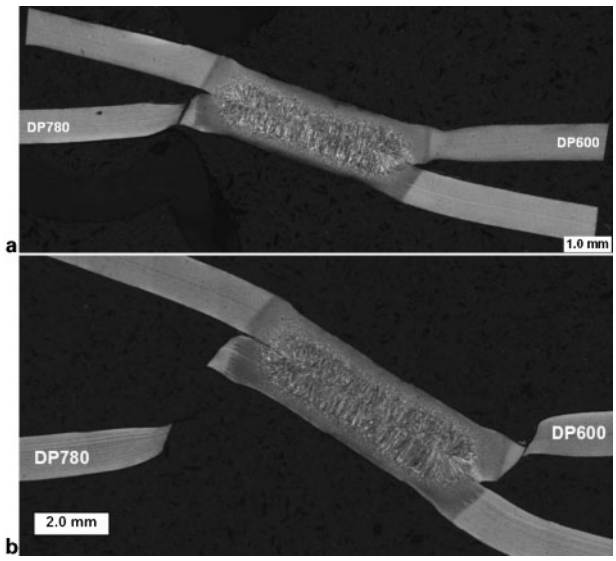

11 Cross-section of DP600–DP780 partial lap shear tensile test at: *a* 2·0 mm displacement, just after peak load and *b* 2·4 mm displacement, just after final fracture

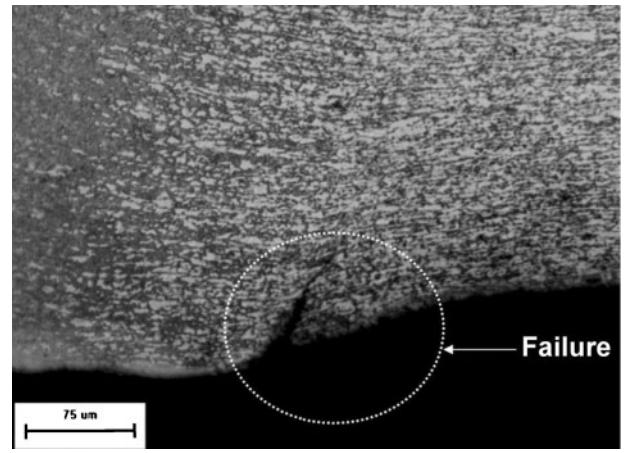

12 Fracture initiation at BM/HAZ boundary in DP600 steel at 2·0 mm of displacement in partial tensile test

tensile tests were completed to facilitate observation of failure initiation. The crosshead was stopped just after the peak load at a displacement of 2·0 mm, and after the final fracture in both sheets at 2·4 mm (Fig. 10). Cross-sections of the partial tensile tests show details of fracture initiation and propagation. Figure 11*a* showed that necking was localised in the HAZs of both the DP600 and DP780 sheet, and that fracture occurred first in the DP780. Upon continued displacement, fracture also occurred just outside of the DP600, as shown in Fig. 11*b*. From Fig. 3, the cross-weld hardness profiles in the outer, subcritical HAZ of the DP780 exhibited softening as a result of martensite tempering. Softening served to locally lower the yield strength in the DP780 HAZ and resulted in a strain concentration in the softened region when the yield strength was exceeded.[4,7] The DP600 did not show any measurable softening in the HAZ; however, there was significant necking observed. The hardness and strength of the DP600 BM was still lower than the softened region in the DP780 HAZ, thus it is expected that the yield strength of the DP600 was exceeded first; however, due to work hardening, strain was transferred to the DP780 HAZ and necking was a result of strain concentration. Softening in the HAZ of the DP780 helped promote a lower transition weld size, or in other words, HAZ softening promotes a pullout failure mode.

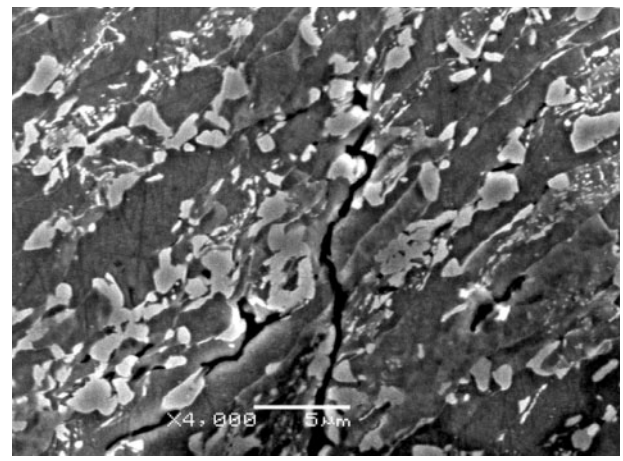

13 Decohesion at martensite/ferrite interface at BM/HAZ boundary in DP600 steel at 2·0 mm of displacement

The peak tensile load of the DP600–DP780 welds at the interfacial pullout transition was similar to the DP600–DP600 welds, and lower than the DP780–DP780 welds. The dissimilar DP600–DP780 weld size was smaller than that of DP600–DP600, so even though the FZ strength was expected to be higher, the failure load was primarily a function of the DP600 BM strength. The optical micrograph in Fig. 12 confirmed the fracture initiation in the BM near the HAZ of the DP600 in the dissimilar combination (DP600–DP780) at 2·0 mm of displacement. At higher magnifications, the SEM image in Fig. 13 shows significant microvoids in the necking region of the DP600. Microvoids are associated with decohesion of the ferrite-martensite interface or separation of adjacent particles due to local deformation generated at the necking (ductile) region.[24] Through thickness failure in both sheets was observed with further displacement (2·4 mm). Despite softening in the HAZ of the DP780, the transition peak failure loads of the DP780–DP780 welds were higher than the DP600–DP780 combination, which was function of larger weld size, higher FZ strength and higher BM/HAZ strength.

Conclusions

1. The microstructure and hardness of the FZ in dissimilar welds with DP600 paired to HSLA, DP780 and TRIP780 were dependent upon the alloy level of the FZ resultant from dilution with the paired material. Increasingly harder microstructures were observed as the alloying level of the paired steel increased. A predominantly martensitic microstructure was observed with some sideplate structures also present in the DP600–HSLA combination.

2. For similar weld size, a pullout failure mode was generally observed in dissimilar welds with DP600 paired to other AHSS compared to an interfacial failure mode for DP600 welded to itself. The weld performance in lap shear and cross-tension testing was generally a function of the BM strength. Weld strength in lap shear loading increased with increasing BM strength, while cross-tension weld strength decreased.

3. In comparison of interfacial to pullout failure transition for DP600, DP780 and DP600–DP780, it was found that the transition weld size was driven lower for the dissimilar combination. Pullout failure modes in DP600–DP780 were promoted by increased FZ strength. Pullout failure modes in DP600–DP780 were promoted by HAZ softening.

4. Heat affected zone softening reduced the strength of the HAZ and resulted in strain localisation and primary failure in the DP780 sheet in lap shear tensile testing of the DP600–DP780 dissimilar welds.

Acknowledgements

The authors would like to acknowledge the funding from Auto21, one of the Networks of Centres for Excellence supported by the Canadian Government. The authors also want to acknowledge the support from the Mexican National Council for Science and Technology (CONACYT) and the Autonomous University of Zacatecas.

References

1. Committee on Automotive Applications: 'AHSS – application guidelines'; 2006, Washington DC, International Iron and Steel Institute.
2. H. Y. Zhang and J. Senkara: 'Resistance welding fundamental and applications', 1–2; 2006, Boca Raton, FL, CRC Press.
3. M. I. Khan, M. L. Kuntz, E. Biro and Y. Zhou: *Mater. Trans. JIM*, 2008, **49**, (7), 1629–1637.
4. P. Ghosh, P. Gupta, Ramavtar and B. Jha: *Weld. J.*, 1991, **70**, (1), 7–14.
5. W. Tong, H. Tao, X. Jian, N. Zhang, M. Marya, L. Hector and X. Q. Gayden: *Metall. Mater. Trans. A*, 2005, **36A**, 2651–2669.
6. M. I. Khan, M. L. Kuntz and Y. Zhou: *Sci. Technol. Weld. Joining*, 2008, **13**, 49–59.
7. S. Zuniga and S. D. Sheppard: *Fatigue Fract. Mech.*, 1997, **27**, 469–489.
8. M. Marya and X. Q. Gayden: *Weld. J.*, 2005, **84**, (12), 197–204.
9. M. Marya, K. Wang, L. G. Hector and X. Gayden: *J. Manuf. Sci. Technol.*, 2006, **128**, 287–298.
10. M. Pouranvari, H. R. Asgari, S. M. Mosavizadch and P. H. Marashi: *Sci. Technol. Weld. Joining*, 2007, **12**, 217–225.
11. M. Kuo and J. Chiang: *SAE Trans.*, 2004, **113**, (5), 67–77.
12. M. I. Khan, M. L. Kuntz, P. Su, A. Gerlich, T. North and Y. Zhou: *Sci. Technol. Weld. Joining*, 2007, **12**, 175–182.
13. M. Marya and X. Q. Gayden: *Weld. J.*, 2005, **84**, (11), 172–182.
14. M. Kuo and A. Wexler: Proc. Conf. AWS SMWC XI, Detroit, MI, USA, May 2004, RoMan Engineering Services Inc., Paper 5·6.
15. M. Milititsky, E. Pakalnins, C. H. Jiang and A. Thompson: 'On characteristics of DP600 resistance spot welds', SAE Report 2003-01-0520, Warrendale, PA, USA, 2003.
16. L. E. Svensson: *Weld. World*, 2004, **48**, 31–35.
17. N. Yurioka, H. Suzuki, S. Ohshita and S. Saito: *Weld. J.*, 1983, **62**, 147–153.
18. RWMA: 'Resistance welding manual', 4th edn; 2003, Philadelphia, PA, RWMA, 18-1–18-14.
19. 'Recommended practices for test methods for evaluating the resistance spot welding behavior of automotive steels', ANSI/AWS/SAE/D8·9–97, AWS, Miami, FL, USA, 1997.
20. V. H. Baltazar, I. Khan, M. L. Kuntz and Y. Zhou: Proc. MS&T Conf., Detroit, MI, USA, September 2007, AcerS/AIST/ASM/TMS, Paper 0217.
21. H. Oikawa, T. Sakiyama, T. Ishikawa, G. Murayama and Y. Takahashi: *Nippon Steel Tech. Rep.*, 1995, (95), 39–45.
22. Y. J. Chao: *ASME J. Eng. Mater. Technol.*, 2003, **125**, 1–8.
23. S. H. Lin, J. Pan, S. R. Wu, T. Tyan and P. Wung: *Int. J. Solids Struct.*, 2002, **39**, 19–39.
24. M. Erdogan and S. Tekeli: *Mater. Des.*, 2002, **23**, 597–604.